



Sediment mobilization by bottom trawls: a model approach applied to the Dutch North Sea beam trawl fishery

A. D. Rijnsdorp ^{1*}, J. Depestele², P. Molenaar¹, O. R. Eigaard³, A. Ivanović⁴, and F.G. O'Neill⁵

¹Wageningen Marine Research, Wageningen University and Research, AB IJmuiden, the Netherlands

²Flanders Research Institute for Agriculture, Fisheries and Food (ILVO), 8400 Oostende, Belgium

³National Institute of Aquatic Resources (DTU AQUA), Technical University of Denmark, Lyngby, Denmark

⁴School of Engineering, Fraser Noble Building, University of Aberdeen, UK University of Aberdeen, Aberdeen, UK

⁵DTU Aqua, National Institute of Aquatic Resources, North Sea Science Park, Hirtshals, Denmark

*Corresponding author: tel: +31 317487191; e-mail: adriaan.rijnsdorp@wur.nl.

Rijnsdorp, A. D., Depestele, J., Molenaar, P., Eigaard, O. R., Ivanović, A., and O'Neill, F.G. Sediment mobilization by bottom trawls: a model approach applied to the Dutch North Sea beam trawl fishery. – ICES Journal of Marine Science, 78: 1574–1586.

Received 2 December 2020; revised 22 January 2021; accepted 5 February 2021; advance access publication 7 April 2021.

Bottom trawls impact the seafloor and benthic ecosystem. One of the direct physical impacts is the mobilization of sediment in the wake of trawl gear components that are in contact with or are close to the seabed. The quantity of sediment mobilized is related to the hydrodynamic drag of the gear components and the type of sediment over which they are trawled. Here we present a methodology to estimate the sediment mobilization from hydrodynamic drag. The hydrodynamic drag of individual gear components is estimated using empirical measurements of similarly shaped objects, including cylinders, cubes, and nets. The method is applied to beam trawls used in the Dutch North Sea flatfish fishery and validated using measurements of beam trawl drag from the literature. Netting contributes most to the hydrodynamic drag of pulse trawls, while the tickler chains and chain mat comprise most of the hydrodynamic drag of conventional beam trawls. Taking account of the silt content of the areas trawled and the number of different beam trawl types used by the fleet, sediment mobilization is estimated as 9.2 and 5.3 kg m⁻² for conventional 12 m beam and pulse trawls, respectively, and 4.2 and 4.3 kg m⁻² for conventional 4.5 m beam and pulse trawls.

Keywords: beam trawl, benthic ecosystem, chain mat, electro trawls, hydrodynamic drag, pulse trawl, tickler chains, trawling impact

Introduction

There is a great diversity of seafloor habitats that are related to the geological history and contemporary physical and biological processes of the sea (Harris and Baker, 2012). The seafloor habitats are affected by the activities of benthic organisms that may create biogenic structures or may be responsible for the bio-irrigation and bioturbation of soft sediments (Bolam *et al.*, 2017). Seafloor communities play an important role in the biogeochemical processes in the seabed, such as the decomposition of organic material and the recycling of nutrients to the overlying waters (Soetaert and Middelburg, 2009; Provoost *et al.*, 2013).

Bottom trawling may disturb the structure of seafloor habitats and the functioning of benthic ecosystems (Jennings and Kaiser, 1998). Trawling affects the composition and biomass of the benthic community (Sciberras *et al.*, 2018) and can destroy biogenic habitats, such as coral reefs (Clark *et al.*, 2016). Trawling can also trigger secondary effects through the food web, which may affect the productivity of fish stocks (Collie *et al.*, 2017; van de Wolfshaar *et al.*, 2020).

Bottom trawling mixes the top layer of the sediment and mobilizes fine sediments from the sea floor into the water column (Lucchetti and Sala, 2012). Both fining (Trimmer *et al.*, 2005)

© International Council for the Exploration of the Sea 2021.

This is an Open Access article distributed under the terms of the Creative Commons Attribution License (<http://creativecommons.org/licenses/by/4.0/>), which permits unrestricted reuse, distribution, and reproduction in any medium, provided the original work is properly cited.

and coarsening (Palanques *et al.*, 2014; Mengual *et al.*, 2016) of the sediment have been attributed to trawling, as well as chronic organic matter depletion (Pusceddu *et al.*, 2014; Paradis *et al.*, 2019). Sediment mobilization will affect turbidity and may result in smothering of benthic animals (Jones, 1992) and the clogging of the feeding organs of suspension-feeding organisms (Rhoads, 1974). The effects of bottom trawling on biogeochemical dynamics, however, remain relatively understudied. Trawling has been linked with enhanced carbon mineralization rates due to organic matter priming (van de Velde *et al.*, 2018) and/or trawl-induced increases in organic material (Polymenakou *et al.*, 2005; Pusceddu *et al.*, 2005; Palanques *et al.*, 2014; Sciberras *et al.*, 2016). These results seemingly in contrast with the findings of acute organic matter depletion (Mayer *et al.*, 1991; Brylinsky *et al.*, 1994; Watling *et al.*, 2001) and reduced mineralization rates after acute trawling (Tiano *et al.*, 2019), highlighting the lack of knowledge on this topic and the need for further investigation (de Borger *et al.*, 2020).

Recently, methods have been developed to quantify the impact of bottom trawling on seafloor habitats and biomass and community composition of benthos in soft sediment habitats that can be used at the scale of management areas and ocean basin (Pitcher *et al.*, 2017; Rijnsdorp *et al.*, 2020b; Mazor *et al.*, 2021). The impact can be estimated by combining information on the spatial distribution and intensity of trawling activities (Eigaard *et al.*, 2017; Amoroso *et al.*, 2018) with information on the design and dimensions of the bottom trawl gears used (Eigaard *et al.*, 2016) and with information on modelled sensitivities of different habitats (Rijnsdorp *et al.*, 2018; Hiddink *et al.*, 2019). High resolution data on trawling activity have become available from Vessel Monitoring System (VMS) and Automatic Identification System (Hintzen *et al.*, 2012; Lambert *et al.*, 2012; Oberle *et al.*, 2016). The impact of bottom trawling differs among fishing gears and habitats and is related to the depth of penetration of the fishing gear into the sediment (Hiddink *et al.*, 2017; Sciberras *et al.*, 2018).

A method to quantify the mobilization of fine sediment of different gear types that can be used at the scale of ecoregions and management areas is lacking. The aim of this paper is to fill this gap in the tool box of trawling impact methodologies. The developed method builds on the knowledge that sediment mobilization

is mainly due to the turbulence behind the gear, which brings fine particles into suspension. The amount of sediment mobilized is a function of the hydrodynamic drag of the trawl and the percentage of fine particles of the sediment (O'Neill and Ivanović, 2016; O'Neill and Summerbell, 2016). We apply a mechanistic approach that decomposes a trawl into its main components (Paschen *et al.*, 2000; Eigaard *et al.*, 2016) and estimate the hydrodynamic drag and sediment mobilization of each component from its shape, frontal surface area and speed. The sediment mobilized by the whole gear is estimated for a range of seafloor habitats by sum up the sediment mobilization of the individual components.

The developed method is applied to the Dutch beam trawl fishery for flatfish. Beam trawls are used in the North Sea and other sea areas in the northeast Atlantic to target flatfish species, in particular sole *Solea solea* (Horwood, 1993; Engelhard, 2008; Rijnsdorp *et al.*, 2008; Polet and Depestele, 2010). Concerns have been raised about the ecological impact of beam trawls because of the deployment of chains to chase sole from the seabed (Jennings and Kaiser, 1998; Kaiser *et al.*, 2016). To reduce the impact of the beam trawl fishery on the sea bed and reduce fuel use, an innovative pulse trawl has been developed in which mechanical stimulation by tickler chains is replaced with electrical stimulation (Haasnoot *et al.*, 2016; Poos *et al.*, 2020). Electrical stimulation induces a cramp response in the fish that inhibits their ability to escape from the approaching trawl (Soetaert *et al.*, 2015; de Haan *et al.*, 2016). Pulse trawling proved to be particularly efficient for sole, which cramp in a U-shape making them easy to catch (Soetaert *et al.*, 2016; Poos *et al.*, 2020). Here we compare the sediment mobilization by the conventional tickler chain and chain mat beam trawls with the sediment mobilization by innovative pulse trawls as used in the Dutch fleet. The validity of the model approach is tested and discussed by comparing the modelled hydrodynamic drag with *in situ* measurements of conventional beam trawls from the literature.

Material and methods

Beam trawl types used for catching flatfish

Different types of beam trawls are used in the northeast Atlantic. The horizontal net opening of a beam trawl is fixed by either a traditional beam that is resting on two shoes (Figure 1a and b) or

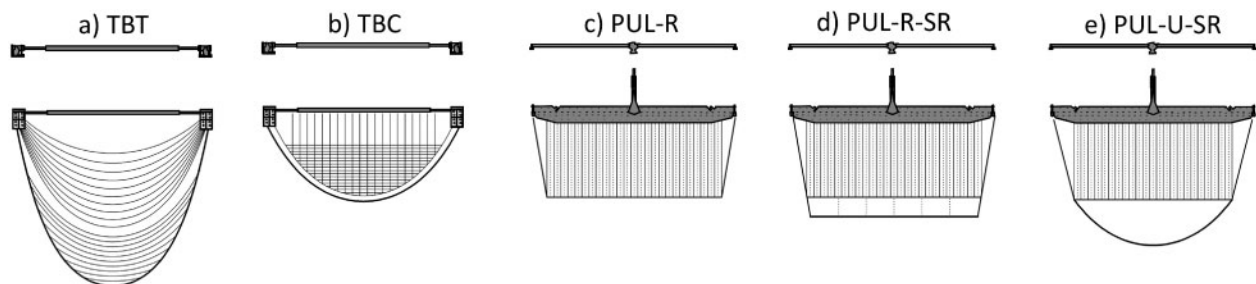


Figure 1. Drawing of the different types of 12 m beam trawls used in the fishery for sole in the North Sea: (a) conventional beam trawl (TBT) with beam, shoes, and tickler chains attached to either the shoes (shoe ticklers) or ground rope (net ticklers); (b) conventional chain mat beam trawl (TBC) with perpendicular and longitudinal chains attached between the beam and second ground rope; (c) pulse trawl with rectangular ground rope (PUL-R) with electrodes (thin lines) and tension relief cords (dashed lines) attached between the Sumwing and the ground rope; (d) pulse trawl with rectangular ground rope and lighter sole rope and sole panel (PUL-R-SR) with electrodes (thin lines) and tension relief cords (dashed lines) attached between the Sumwing and the sole rope and five additional tension relief cords between the Sumwing and the ground rope; (e) pulse trawl with U-shaped ground rope and lighter sole rope and sole panel (PUL-U-SR) with electrodes (thin lines) and tension relief cords (dashed lines) attached between the Sumwing and the sole rope. Top panels show the frontal view of the beam and wing. Bottom panels show the bottom view. Note that TBT, PUL-R, PUL-R-SR, and PUL-U-SR can be combined with a beam and a Sumwing.

by a wing (Figure 1c–e). The wing avoids the use of trawl shoes, improves the streamline, and reduces both the hydrodynamic drag and fuel consumption (van Marlen et al., 2009; Taal and Klok, 2014). The nose of the wing, attached to the front side in its centre, follows the seafloor topography to maintain the position of the wing just above the seafloor (Polet and Depestele, 2010). The wing (Sumwing) is a recent innovation that replaced the traditional beam with trawl shoes in many of the vessels of the Dutch fleet since its introduction in 2008 (www.agrimatie.nl, visited on 21 October 2020). During the transition from conventional beam trawling to pulse trawling, the fishing effort of the Dutch fleet decreased from about 480 10³ h in 2009 (all conventional beam trawling) to 400 10³ h in 2017 (25% conventional beam trawl and 75% pulse trawl) (Rijnsdorp et al., 2020a).

According to the type of stimulation beam trawls can be classified as conventional beam trawls (Figure 1a and b), that use mechanical stimulation to chase flatfish out of the sediment, and pulse trawls (Figure 1c–e), that use electrical stimulation to immobilize the fish. In conventional beam trawls, the flatfish are stimulated by tickler chains, attached to the shoes/wing or ground rope (TBT, Figure 1a), or by a chain mat comprising of a matrix of longitudinal and transverse chains between the ground rope and the beam (TBC, Figure 1b) (de Groot and Lindeboom, 1994). The chain mat beam trawl is used on rough grounds and prevents large stones from entering the net.

Pulse trawls deploy a matrix of electrode arrays running from the wing or beam to the ground rope (Figure 1c–e). In order to operate properly, the electrodes need to be of equal length and are equally spaced over the width of the trawl (Soetaert et al., 2019). Tension relief cords are deployed between the wing or beam and the ground rope to release the tension on the electrodes and maintain the ground rope shape (Depestele et al., 2019). Different types of ground ropes and net designs were developed to accommodate a rectangular-shaped electric field of which three are commonly deployed in the fishery. The PUL-R type deploys a rectangular shaped ground rope (Figure 1c), PUL-R-SR deploys a rectangular ground rope (Figure 1d), and PUL-U-SR uses a U-shaped ground rope (Figure 1e). The PUL-R-SR and PUL-U-SR types have an additional ground rope (sole-rope) and a netting panel between the two ground ropes. In contrast to the electrodes, which have physical contact with the sea floor, tension relief cords generally do not touch the sea floor (Depestele et al., 2019).

The beam trawl fleet comprises small (maximum engine power of 221 kW) and large vessels (maximum engine power of 1467 kW) that operate under different management constraints. Small vessels are allowed to fish for flatfish with two beam trawls of up to 4.5 m within the 12 nautical mile zone, although some vessels also fish outside the 12 nm zone with 7 or 8 m beam trawls. Large vessels are allowed to fish outside the 12 nm zone with two 12 m beam trawls. All of the small vessels fishing with a pulse trawl use the PUL-R rigging type, mostly in combination with a beam. Among the large vessels, 35% use the PUL-R type, 18% use the PUL-R-SR type, and 47% use the PUL-U-SR type. About two-thirds of the large pulse trawl vessels use a wing and one-third a traditional beam to fix the horizontal net opening. Towing speed differs across gears and fleet segments (Poos et al., 2020). Towing speeds were calculated for the study period 2009–2017 using VMS, which records the vessel ID, speed, and position with a time interval of 2 h or less, following the methodology described in Hintzen et al. (2012). The fishing effort of the Dutch beam trawl fleet is dominated by large vessels, which contribute

to 94.6% of the total area swept in the study period of conventional beam trawls and 87.6% of pulse trawls.

Gear components

The hydrodynamic drag was estimated for the gear components that are in contact with the seafloor, or towed just above the seafloor: ground gear, tickler chains, chain mat, electrodes and tension relief cords, bottom panels of the net, shoes of the beam trawl, and the nose of the wing. Data were compiled on the number, length, angle of attack, and frontal surface area of the various components as described in the Supplementary material SM1 and are representative for the flatfish fisheries in the period 2010–2018.

Data on conventional tickler chain and chain mat beam trawls were available from enquiries on-board fishing vessels and with net makers and from direct measurements of chain mat beam trawls in Belgian and Dutch harbours. The enquiry data were complemented with data obtained from the literature (Fonteyne and Polet, 1992; de Groot and Lindeboom, 1994; van Marlen et al., 2014) and from experiments on the impact of flatfish trawls on the seabed (Depestele et al., 2016, 2019) and the European wide gear inventory of the BENTHIS project (Eigaard et al., 2016). Information on the pulse trawl gear was available from the “Technical Dossiers” (TD) of the pulse trawl vessels providing information on the pulse system, gear type, ground gear, and net panels and from the literature (van Marlen et al., 2014; Depestele et al., 2016, 2019; Soetaert et al., 2019).

Hydrodynamic drag

Introduction

The hydrodynamic drag of a body is a function of the projected frontal area A_f (m²) of the body in the towing direction, the towing speed U (ms⁻¹), the hydrodynamic drag coefficient of the body c_D , and the density of water ρ (kg.m⁻³) and is expressed as:

$$D = 0.5\rho A_f U^2 c_D. \quad (1)$$

The hydrodynamic drag coefficient is a dimensionless quantity that depends on the geometry of the body, the Reynolds number, and the surface roughness. There has been much research done on the drag coefficient of bodies with basic geometric shapes such as circular cylinders, cubes, and spheres and many experiments have been carried out to measure them (Hoerner, 1965). These experiments have usually been carried out for bodies that are towed obliquely. Hoerner (1965) shows that when cylinders are towed at an angle to the flow, the “cross-flow” principle applies and that the hydrodynamic pressure forces only correspond to the velocity component in the direction normal to their axis. He demonstrates that the resulting drag on a cylindrical section of diameter d , length l , and angle of attack α is given by:

$$Dc = 0.5\rho U^2 dl c_D \sin^3(\alpha), \quad (2)$$

where c_D is the drag coefficient of the component when it is towed obliquely (i.e. $\alpha = 0$). This formulation is appropriate when the cylinder is relatively long i.e. when $l \gg d$, and here we use it to estimate the drag of sections of chains and ground gears.

To apply these equations, we need to know the towing speed, the drag coefficient, the frontal area, and the angle of attack of the individual components. As mentioned above, the towing speed

Table 1. Gear components, hydrodynamic drag coefficient, and equation number used to estimate the hydrodynamic drag.

Gear component	<i>cd</i>	Equation
Shoe	1.05	1
Nose	1.1	1
Beam	1.1	1
Ground rope	1.1	2
Tickler chain	2.3	2
Electrode in water	1.1	2
Electrode on seafloor	0.8	1
Tension relief cord	1.1	2
Net panels	–	10

of a particular gear can be estimated from VMS data. Very little is known, however, regarding the drag coefficients of beam trawl components. The Reynolds numbers of many of the components are in the subcritical flow range (10^3 – 10^5), where the boundary layer flow is laminar, there is flow separation and the principle contribution to the hydrodynamic drag is from the pressure differential over the components surface. Hence we use drag coefficients, which are characteristic of this flow regime. For chains, we use values calculated by Xu and Huang (2014), and for some of the ground gear components, we use measurements made by O'Neill and Summerbell (2016). Where measurements are not available we use those that have been made for similarly shaped objects such as cylinders, disks, cubes, and spheres and which have Reynolds numbers in the subcritical flow range (Hoerner, 1965). Table 1 shows the drag coefficients used for the different beam trawl gear components. No information on the variance in drag coefficients is readily available.

The frontal area and angle of attack of components such as the shoes, beam, and nose or wing are well defined and readily measurable, whereas those for components such as the ground gears, tickler chains, chain mats, and electrodes are more variable and depend on the rigging of the gear. Therefore, we need to look at these components in more detail.

Catenary

A chain or ground rope that is hanging freely from two points forms a catenary and this curve is often used to approximate the geometry of ground ropes and tickler chains as they are towed across the seabed (Sangster and Breen, 1998). The x and y coordinates of a catenary of length (L) and distance (S) between the hanging points is given by:

$$y = a \cosh\left(\frac{x}{a}\right), \quad (4)$$

where a is a solution to

$$2a \operatorname{asinh}\left(\frac{L}{2a}\right) = S \quad (5)$$

and can be determined using optimization routines such as the R function “optimize” when L and S are known (Brent, 1973).

Ground gear

We assume that the U-shaped ground gears of TBT and TBC (Figure 1a and b) form catenaries where L is the ground gear length and S is the beam width. To estimate their hydrodynamic drag, we subdivide them into 100 piecewise linear segments and calculate the drag of each segment using equation (2).

The ground gear of the PUL-R and PUL-R-SR type comprises two (almost) longitudinal sections and a transverse section (PUL-R) (Figure 1c). The ground gear of the PUL-R-SR and PUL-U-SR type (Figure 1d and e) comprises two (almost) longitudinal sections, a transverse or U-shaped section, and an additional transverse sole rope. Given the length of the ground gear sections, the angle of attack of the longitudinal sections was calculated by geometry. The U-shaped section was assumed to form a catenary. The hydrodynamic drag of the ground gear was calculated as the sum of the drag of the ground gear sections using equations (1) and (2).

Tickler chains

We also assume that the tickler chains form catenaries. Tickler chains can be grouped into two main categories: those that are attached to the shoes (shoe ticklers) and those that are attached to the ground gear or footrope (net ticklers). The distance between the attachment points of shoe ticklers is the beam width but for the net ticklers it varies (Figure 1a). There is little information available on the length of the net ticklers and the distance between their attachment points. Nevertheless, given that they are deployed such that they are distributed evenly between the ground rope and the beam, we estimated the length of chain i to be:

$$L_i = l_{min} + (i - 1) * (l_{max} - l_{min}) / (n - 1), \quad (6)$$

where n = number of tickler chains and l_{max} (l_{min}) = median value of the largest (smallest) length observed (shoe tickler: l_{max} =24 m and l_{min} =18 m; net tickler: l_{max} =13 m and l_{min} =4 m). For the net ticklers, the position of the attachment points was estimated from the intersection of the ground gear and the tickler chain catenaries. As for the ground gears, the tickler drag was found by estimating the drag of 100 piecewise linear section using their respective length l and angle of attack α in equation (2).

Chain mats

A chain mat comprises of a matrix of longitudinal and transverse chains that are attached to the ground rope and the beam. Information was available on the number and chain link diameter of the longitudinal and transverse chains but not on their length. The lengths of the chains were estimated from the vertical distances between the point of attachment along the ground gear catenary and the beam (longitudinal chains) and the horizontal distances between the points of attachment (transverse chains). The points of attachment of the chains along the ground rope catenary were determined by distributing them equally over the width of the trawl. The drag of the transverse chains was estimated using equation (1) and that of the longitudinal chains using equation (2) where $\alpha = \operatorname{asin}(h/l_{chain})$ where h = height of the beam above the sea bed and l_{chain} = chain length.

Electrode arrays and tension relief cords

Electrodes and tension relief cords are attached to the beam or Sumwing and run in the towing direction. The conductor section of the electrodes is in contact with the seabed; hence, the length above the seabed is the total length of electrode array (l_{tot}) minus the length of the conductors and isolator parts (l_{cond}). The angle of attack of this section is given by:

$$\alpha_e = \text{asin}(h/(l_{tot}-l_{cond})). \quad (7)$$

Additional drag is generated by the isolating parts that generally have a larger diameter (d_1) than the conducting parts of the electrode array (d_2). This component is estimated as the product of the number of conducting parts (n_c) and the difference in frontal surface areas of the isolator and the conductor.

$$A = n_c \pi (d_1^2 - d_2^2) / 4 \quad (8)$$

To estimate the drag of the tension relief cords, we assume that they run in a straight line between the beam or Sumwing at height h and the ground rope, and consequently their angle of attack is:

$$a_{trc} = \text{asin}(h/l_{trc}). \quad (9)$$

A drag coefficient of 0.8, applicable for blunt-shaped cylinders in axial flow (Hoerner, 1965), is used for the electrode part that is in contact with the sea floor. For the other part and the tension relief cords the drag coefficient of 1.1 is used for cylinders.

Net panels

There has been a lot of research undertaken on the hydrodynamic drag of netting panels at specific angles of attack and for given solidity and hanging ratios (Zhou et al., 2015; Tang et al., 2019). To use that information here would require a detailed understanding of the netting geometry as the gear is being fished, which in general is not available. Hence we use the results of Reid (1977), who found the following dependence of netting drag on the twine surface area (A) and towing speed (U) from experimental trials:

$$Dn = \frac{0.5\rho*U^2*A*0.643}{1 + 0.923U}. \quad (10)$$

The twine surface area is estimated from:

$$A = (N_t + N_b)N_dMd, \quad (11)$$

where N_t is the number of meshes on the top row of a panel, N_b the number on the bottom row, N_d the number along the length of the panel, M the mesh size, and d the twine diameter (Ferro, 1981). The diameter of double braided twine is assumed to be 1.64 times the diameter of one of the component single twines.

Total gear

To estimate the total hydrodynamic drag of a gear, we sum the contributions from each of the individual gear components. Thus, we implicitly assume that there is no hydrodynamic interaction between components and that their contribution is additive.

To assess the validity of this approach, we compare our hydrodynamic drag estimates with *in situ* measurements of beam trawl drag. Three studies are available in which the total drag of an 11 and 12 m commercial beam trawl and 4 m chain mat trawl was measured over a range of towing speeds and the gear dimensions. Blom (1982, 1990) studied the drag of a tickler chain beam trawl and estimated the separate contribution of the shoe tickler chains and net, whereas Fonteyne and co-workers (in Paschen et al., 2000) studied the contribution of the chain mat plus ground rope and net.

Sediment mobilization of different beam trawl types

Sediment mobilization was estimated for each gear type taking account of the mean annual swept area and the silt fraction in the fished 1 min latitude \times 1 min longitude grid cells of the fishing area (Figure 2). The analysis was restricted to beam trawl fishing trips for sole in the North Sea between 51°N and 55°N west of 5°E and 56°N east of 5°E and distinguishing between small (engine power \leq 221 kW) and large (engine power $>$ 221 kW) vessels. For the conventional beam trawls (TBT, TBC), data were from the years 2009 to 2010 before the transition to pulse trawling. For the pulse beam trawls data were from 2016 to 2018 after the transition (Poos et al., 2020). Silt fractions were taken from Wilson et al. (2018) who provides mud% at 0.125° longitude by 0.125° latitude.

O'Neill and Summerbell (2011, 2016) measured the sediment mobilization by individual gear components (otter trawl door, rubber disc ground gear, rock hopper ground gear) on a range of different sediment types with silt fractions between 0.02 and 0.69. The amount of sediment mobilized per square metre of seabed swept by each gear component (m_c in $\text{kg}\cdot\text{m}^{-2}$) is:

$$m_c = 2.602s_f + 1.206*10^{-3}D_c + 1.321*10^{-2}s_fD_c, \quad (12)$$

where D_c ($\text{N}\cdot\text{m}^{-1}$) is the hydrodynamic drag generated by the gear component and s_f is the silt fraction of the sediment (O'Neill and Ivanović, 2016). This equation is applicable to any gear component towed across the seabed and is used here to estimate the sediment mobilized by those of the beam trawls.

The components were grouped into four major categories: (i) ground gear; (ii) bottom net panels; (iii) shoes of the beam trawl or nose of the Sumwing; (iv) tickler chains, chain mat or electrodes, and tension relief cords. The hydrodynamic drag of the individual gear components was estimated by applying the equations described above to the dimensions of the bottom gear components summarized in the Supplementary material SM1. The total amount of sediment mobilized by each type of beam trawl was estimated by summing the amount mobilized by each individual gear component using equation (12) in order not to extrapolate too far outside the range of the hydrodynamic drag (50–600 $\text{N}\cdot\text{m}^{-1}$) in the experiments of O'Neill and Summerbell (2011, 2016). To obtain an estimate of the variability from the gear dimensions, the hydrodynamic drag of each component was bootstrapped 1000 times from a normal distribution based on the mean and standard deviation of the dimensions of the sampled gear components. For each D_c , the mean m_c was estimated by randomly drawing 1000 silt fractions from the observed frequency distribution of silt fraction by gear type.

The sediment mobilization of the different beam trawl types were combined to estimate the sediment mobilization of the beam trawl

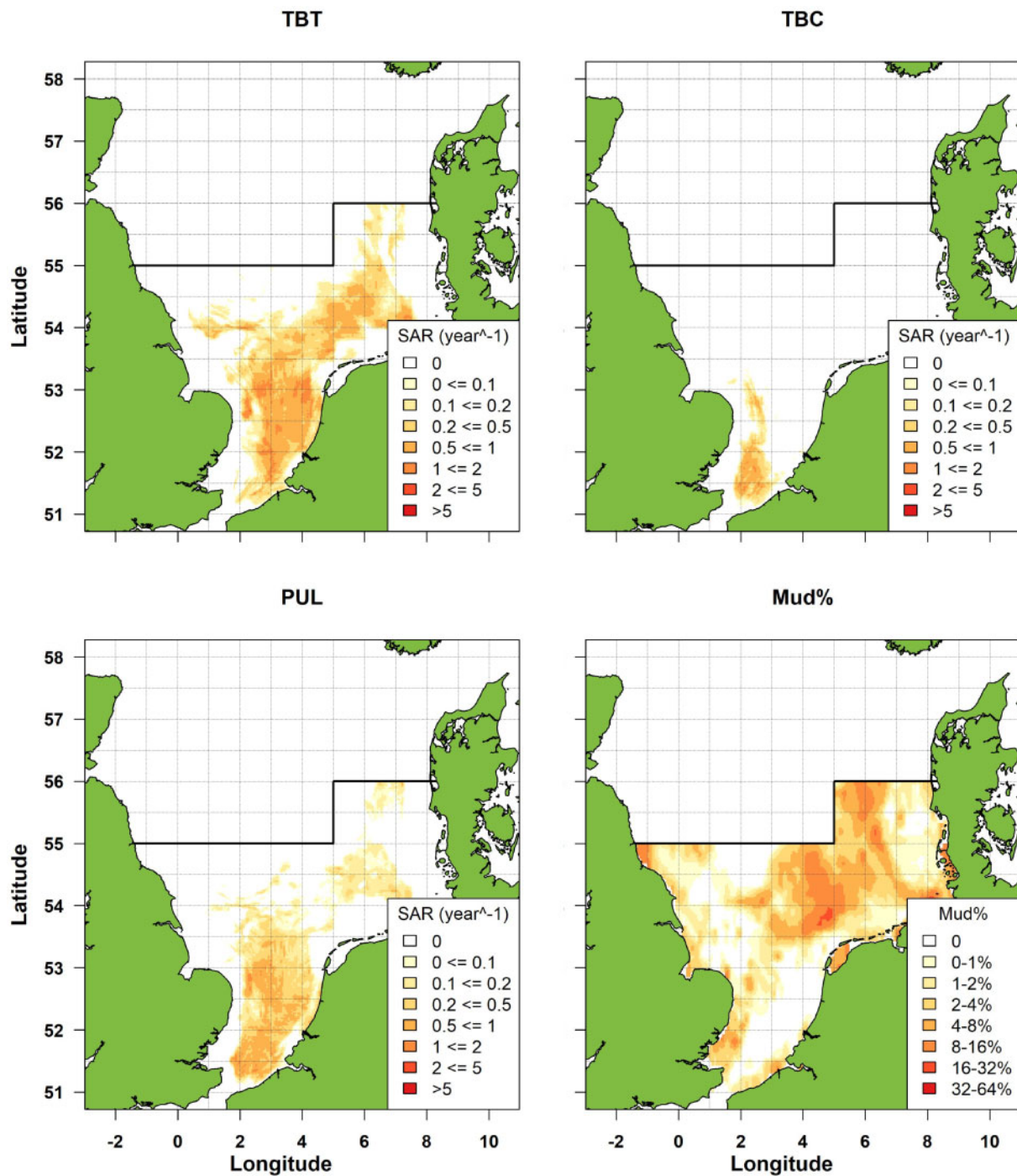


Figure 2. Annual swept area ratio (SAR) of the conventional tickler chain beam trawl (TBT, top left) and chain mat beam trawl (TBC, top right) in the period 2009–2010 and pulse trawl (PUL, bottom left) in the period 2016–2018 and the mud percentage (bottom right) according [Wilson et al. \(2018\)](#) in the sole fishing area south of the horizontal line.

fleet of the Netherlands when using either the conventional beam trawl or innovative pulse beam trawl by taking account of the proportion of each gear type in the fleet ([Table 2](#)).

Results

Hydrodynamic drag of different beam trawls

Large vessels tow their TBT at an average speed of 3.25 m s^{-1} as compared to $2.48\text{--}2.57 \text{ m s}^{-1}$ for different types of pulse trawls

([Table 2](#)). The difference in towing speed between gear types is less in small vessels: 2.59 and $2.34\text{--}2.39 \text{ m s}^{-1}$, respectively. The towing speed of TBC trawlers is slightly lower than TBT trawlers but higher than PUL trawlers. The mean towing speed of PUL trawlers does not differ between rigging types.

The estimated hydrodynamic drag of the different gear components that are in close contact with the seafloor, and therefore relevant when assessing the impact on the mobilization of sediment,

Table 2. Towing speed (m s^{-1}) and sampled number of beam trawl vessels (n) by gear type for the small and large fleet component.

Gear type		Small vessels (≤ 221 kW)			Large vessels (> 221 kW)		
		Mean	SD	n	Mean	SD	n
TBT	Beam/wing	2.59	0.33	51	3.25	0.20	76
TBC	Beam	2.73	0.09	5	3.13	0.11	10
PUL	Beam/wing	2.39	0.12	18	2.52	0.08	57
PUL-R	Beam	2.39	0.13	13	2.52	0.03	5
	Wing	2.34	0.04	3	2.51	0.10	10
PUL-R-SR	Beam	–	–	–	2.47	0.06	2
	Wing	–	–	–	2.48	0.07	9
PUL-U-SR	Beam	–	–	–	2.57	0.01	2
	Wing	–	–	–	2.53	0.09	22

TBT is conventional tickler chain beam trawl, TBC is conventional chain mat beam trawl, PUL-R is a pulse trawl with a rectangular ground gear, PUL-R-SR is a pulse trawl with a rectangular ground gear and an additional sole rope, PUL-U-SR is a pulse trawl and a U-shaped ground gear and additional sole-rope. Gear types are depicted in Figure 1.

Table 3. Hydrodynamic drag (kN m^{-1}) per metre gear width of major gear components of conventional tickler chain and chain mat beam trawl and three types of pulse trawls at the observed towing speeds in Table 2.

Gear component	Small vessels (< 221 kW)			Large vessels (> 221 kW)		
	Mean	SD	n	Mean	SD	n
Tickler chain beam trawl (TBT)						
Ticklers	0.699	0.194	3	2.118	0.352	8
Ground gear	0.135	0.115	2	0.572	0.140	7
Net bottom	1.595	0.805	3	1.967	0.333	12
Shoes	0.019	–	1	0.013	0.002	6
Chain mat beam trawl (TBC)						
Tick_chainmat	0.754	–	1	2.190	0.020	2
Ground gear	0.581	–	1	1.272	0.062	2
Net bottom	1.594	–	1	1.638	0.246	2
Shoes	0.021	–	1	0.012	0.002	6
Pulse trawl: rectangular ground rope (PUL-R)						
Electrodes	0.189	0.024	16	0.273	0.023	18
Ground gear	0.772	0.213	13	0.626	0.051	8
Net bottom	1.641	0.336	3	1.762	0.290	14
Shoes-nose	0.004	0.002	9	0.004	0.002	3
Pulse trawl: rectangular ground rope plus sole rope (PUL-R-SR)						
Electrodes	–	–	–	0.226	0.016	11
Ground gear	–	–	–	0.927	0.310	6
Net bottom	–	–	–	2.135	0.275	2
Shoes-nose	–	–	–	0.004	0.002	3
Pulse trawl: U-shaped ground rope plus sole rope (PUL-U-SR)						
Electrodes	–	–	–	0.235	0.014	26
Ground gear	–	–	–	0.719	0.092	13
Net bottom	–	–	–	2.350	0.258	19
Shoes-nose	–	–	–	0.005	0.001	3

is presented in Table 3. For small vessels, net panels have the largest contribution for all gear types ($1.59\text{--}1.64 \text{ kN m}^{-1}$), followed by the tickler chains (0.70 kN m^{-1}) and chain mat (0.75 kN m^{-1}) for conventional beam trawls and the ground gear for pulse trawls (0.77 kN.m^{-1}). For large vessels, the net panels have the largest contribution for the pulse trawl types ($1.76\text{--}2.35 \text{ kN m}^{-1}$), whereas the tickler chains and chain mat contribute most for the conventional beam trawl gears ($2.12\text{--}2.19 \text{ kN m}^{-1}$).

The largest difference in hydrodynamic drag between gear types was observed for the gear component that plays a role in the stimulation of flatfish. The tickler chains and chain mat used in conventional TBT and TBC had a significantly higher drag

than the electrodes and tension relief cords used in pulse trawls (t -test, $p < 0.01$). Although the electrodes and tension relief cords had a relative small contribution to the drag, significant differences were observed among the PUL types that were related to the different number of electrodes and tension relief cords used (PUL-R $>$ PUL-R-SR and PUL-U-SR; t -test, $p < 0.001$).

The drag of the bottom panels of pulse trawls with an additional sole rope (PUL-U-SR) was significantly higher than that of the pulse trawls without an additional sole rope (PUL-R) (t -test, $p < 0.001$). Significant differences were also observed for the ground gear drag. PUL-U-SR and PUL-R-SR had a significantly higher drag than the traditional TBT and TBC (PUL-U-SR only)

Table 4. Modelled hydrodynamic drag (kN per meter beam width) and sediment mobilization (kg m^{-2} area trawled) of all bottom gear components of conventional beam trawls (TBC—chain mat beam trawl, TBT—tickler chain beam trawl) and innovative pulse trawls (PUL-R, PUL-R-SR, PUL-U-SR) at observed towing speeds from Table 2 and silt content in Figure 3.

Gear type	Small vessels (≤ 221 kW)				Large vessels (> 221 kW)			
	Drag (kN m^{-1})		Sediment mobilization (kg m^{-2})		Drag (kN m^{-1})		Sediment mobilization (kg m^{-2})	
	Mean	SD	Mean	SD	Mean	SD	Mean	SD
Conventional beam trawls								
TBT	2.48	0.79	4.21	1.26	4.64	0.50	9.45	0.97
TBC	2.95	–	4.64	0.04	5.13	0.26	7.01	0.35
Fleet	2.48	0.79	4.18	1.24	4.71	0.52	9.18	1.22
Innovative pulse beam trawls								
PUL-R	2.60	0.40	4.30	0.62	2.66	0.30	4.57	0.49
PUL-R-SR	–	–	–	–	3.30	0.42	5.58	0.68
PUL-U-SR	–	–	–	–	3.31	0.29	5.60	0.46
Fleet	2.60	0.40	4.30	0.62	3.10	0.42	5.28	0.68

The fleet estimates take account of the number of vessels using a particular gear type (Table 2) and the silt content where the gear types operate.

Table 5. Comparison of the modelled hydrodynamic and measured drag at sea (kN m^{-1}) of tickler chains, chain mat + groundrope, and net.

Gear component	Speed (m s^{-1})	Modelled drag (kN m^{-1})	Measured drag (kN m^{-1})			Ratio modelled/measured	Source
			Mean	Lower	Upper		
Tickler chains	3.1	1.31	1.29	1.16	1.44	1.01	Blom (1982)
Tickler chains	3.6	2.68	1.93	1.85	2.01	1.39	Blom (1990)
Net	3.6	3.82	2.47	2.37	2.56	1.55	Blom (1990)
Net	2.5	2.41	1.00	0.91	1.10	2.41	Paschen <i>et al.</i> (2000)
Chain mat	2.5	1.51	1.17	1.06	1.28	1.29	Paschen <i>et al.</i> (2000)

(t -test $p < 0.05$). Among the pulse trawls, PUL-U-SR had a significantly higher ground gear drag than PUL-R (t -test, $p < 0.01$).

The total hydrodynamic drag of the bottom gear components of 12 m pulse trawls used by large vessels was estimated at 3.10 kN.m^{-1} ($SD = 0.42$), 34% lower than the 4.71 kN m^{-1} ($SD = 0.52$) of the combined conventional 12 m TBT and TBC trawls (Table 4). For small vessels, the estimated hydrodynamic drag of 4.5 m pulse trawls (2.60 kN m^{-1} , $SD = 0.40$) does not differ much from conventional 4.5 m beam trawls (2.48 kN^{-1} , $SD = 0.79$).

Comparison with experimental data

The comparison of modelled hydrodynamic drag with experimental measurements in the literature is presented in detail in Supplementary material SM2. Although the experimental values are of combined hydrodynamic and geotechnical drag, we isolate measurements for tickler chains, chain mats and the gear netting at higher speeds (where we assume the contribution of geotechnical drag is minimized). The correspondence for tickler chains and chain mats is reasonably good. The ratio between the modelled and measured drag of Blom (1982, 1990) tickler chains is 1.01 and 1.39, respectively, while the ratio for the chain mat plus ground rope of Paschen *et al.* (2000) is 1.29 (Table 5). The discrepancy is larger for the netting panels, and the modelled drag of Blom (1990) net is 1.6 times higher than the measured drag while that of Paschen *et al.* (2000) is 2.4 times higher.

Sediment mobilization of different beam trawls

The silt fraction of the fishing grounds differs between the gear types (Figure 3) and is relatively high for TBT and low for TBC.

The silt fraction of the fishing grounds of PUL is intermediate. Small vessels, which mainly fish within 12 nautical miles from the coast, trawl sediments with a lower silt fraction when compared to large vessels using the same gear type, except for small TBC trawlers that fish in areas with a slightly higher silt content.

Figure 4 shows the estimated sediment mobilization and the contribution of the main gear components for the gear types taking account of the modelled hydrodynamic drag and the silt fraction distribution of their fishing grounds. Small vessels mobilize between 4.2 and 4.6 kg sediment per square metre sea floor trawled with negligible differences between the gear types (Table 4). Sediment mobilization by large vessels, estimated between 4.6 and 9.4 kg.m^2 , shows large differences between gear types with pulse trawlers mobilizing less sediment ($4.6\text{--}5.6 \text{ kg m}^{-2}$) than conventional beam trawlers ($7.0\text{--}9.4 \text{ kg m}^{-2}$). Among the pulse gear types, PUL-R mobilizes the least sediment, while among the conventional beam trawl types TBT mobilizes more sediment than TBC. The relative contribution of gear components to the sediment mobilization reflects the differences in hydrodynamic drag of gear components by gear type.

Taking account of the proportion of vessels deploying a certain beam trawl type (Table 2), the sediment mobilization of an average vessel of the Dutch beam trawl fleet is estimated at 9.2 kg m^{-2} (95% cl: 6.8–11.6) for large conventional beam trawlers, 74% higher than the 5.3 kg m^{-2} (95% cl: 3.9–6.6) sediment mobilized by pulse trawlers. For small vessels, sediment mobilization of a conventional beam trawler (4.2 kg m^{-2} ; 95% cl: 1.8–6.6) does not differ from a pulse trawler (4.3 kg m^{-2} ; 95% cl: 3.1–5.5). To contextualize these values, if we assume the sediment has relative density of 2.65 and a porosity of 0.4, then 10 kg of sediment

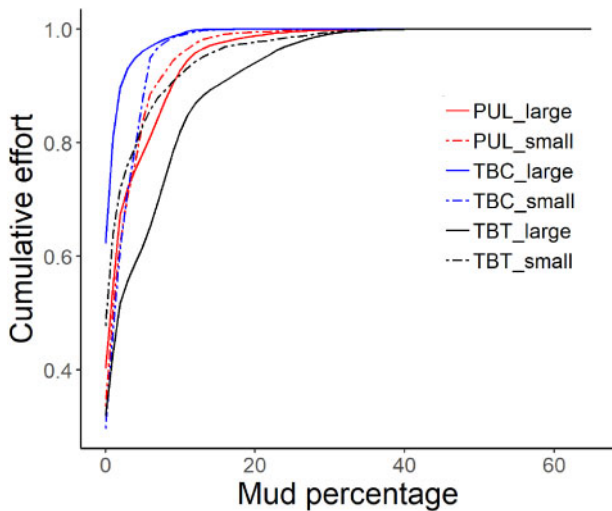


Figure 3. Cumulative distribution of fishing effort (swept area by grid cell) in relation to the mud percentage of the grid cell of the pulse beam trawl (PUL = PUL-R, PUL-R-SR, PUL-U-SR), conventional chain mat beam trawl (TBC), and conventional tickler chain beam trawl (TBT) operated by small and large vessels.

spread over a square metre would have a depth of 6.3 mm (O'Neill and Summerbell, 2011).

Discussion

The application of our methodology to the Dutch beam trawl fishery in the North Sea showed that the innovative pulse trawl that replaced mechanical stimulation of sole by tickler chains or chain mats with electrical stimulation reduced the hydrodynamic drag of the gear and the amount of sediments mobilized in the wake of the trawl of large trawlers but not of small trawlers. Among the conventional beam trawlers, TBC mobilizes less sediments, despite the higher hydrodynamic drag, than TBT because this gear type is used on fishing grounds with low silt content. For large pulse trawlers, which contribute almost 90% of the area swept by the beam trawl fleet, the amount of sediment mobilized per unit area swept is reduced by 34%. Pulse trawls are more efficient to catch the target species sole (Poos *et al.*, 2020) and sweep 28% less sea bed to catch the same amount of sole (Rijnsdorp *et al.*, 2020a). This means that the amount of sediment mobilized by the fleet of large vessels when catching their sole quota will be reduced by 52% ($1 - 0.66 \times 0.72$) when using pulse trawls as compared to conventional beam trawls.

The lower hydrodynamic drag of the pulse trawl is due to the combined effect of the replacement of tickler chains running perpendicular to the towing direction with longitudinal electrodes and the reduction in towing speed. The reduction in hydrodynamic drag is to some extent counteracted by the larger twine surface area of the pulse trawl nets and the larger surface area of the ground rope in pulse trawls. The use of pulse gear requires a rectangular matrix of electrode arrays to generate a stable electric field, constraining the type of ground rope to be used. Three types of ground ropes evolved. The PUL_R type allows fishers to use 26–28 electrode arrays, whereas the PUL_U_SR types allow the deployment of 24 electrode arrays. The smaller number of electrode arrays implies an $\sim 10\%$ narrower electric field, which may reduce the catch efficiency. The reduction in catch efficiency,

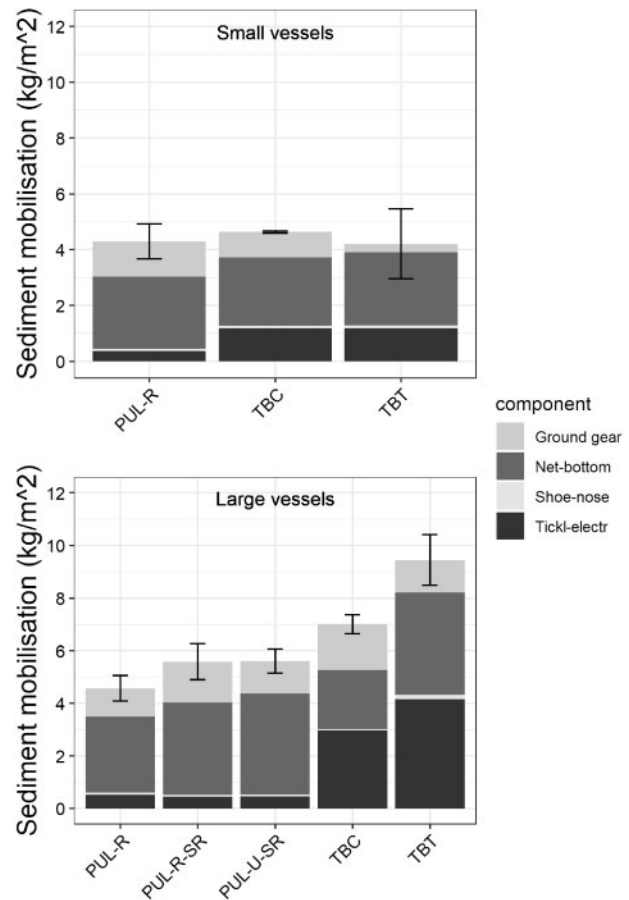


Figure 4. Sediment mobilization (kg m^{-2}) of the gear components of three different pulse trawls (PUL-R, PUL-R-SR, PUL-U-SR), a conventional chain mat beam trawl (TBC), and tickler chain beam trawl (TBT) of small vessels (≤ 221 kW; top panel) and large vessels (> 221 kW; bottom panel). The bars show the standard deviation of the sediment mobilization of the whole gear.

however, may be compensated by the smaller disk diameter of the additional sole-rope, which is expected to better follow the bottom profile and reduce the possibility of the fish escape underneath the sole rope. The different ground rope rigging types used are related to the fishing grounds. Vessels from the northern harbours predominantly use the U-shaped ground rope and sole-rope. In the mid-south and mid-north vessels use a rectangular or U-shaped ground rope and the vessels from the south use rectangular ground ropes.

The overall hydrodynamic drag of tickler chain and chain mat beam trawls is comparable, but drag varies between individual gear components. Chains are contributing nearly equally to the overall hydrodynamic drag while the netting panels are more important in tickler chain trawls. The ground gear is conversely causing a higher drag in chain mat beam trawls.

The results of the current study are representative for the Dutch beam trawl vessels targeting sole and will likely be representative for the entire North Sea beam trawl fleet, which is largely comprised of Dutch owned vessels that were re-flagged to exploit the UK, German, and Belgian quota. The results, however, will be less representative for the Belgian chain mat beam trawlers, where the beam width of large trawlers are varying

between 9 and 12 m, and fishing at lower speeds of 1.9 ($SD=0.4$) to 2.2 ($SD=0.6$) $m\ s^{-1}$ for small and large beam trawlers, respectively (Polet and Depestele, 2010).

We must be aware of the limitations of our approach. The predictions of sediment mobilization are based on the model of O'Neill and Ivanović (2016) who relate the mass of sediment mobilized by a gear component to the silt fraction of the sediment, on which it is being towed, and the hydrodynamic drag of the component. The of silt fraction estimates are interpolated values from a range of data sources compiled by Wilson *et al.* (2018), who produced a synthetic map of the %mud at a resolution of 0.125° by 0.125° . We downscaled these data to the resolution used in our study (0.0166° by 0.0166°), which will influence the spatial accuracy of our approach.

There are also a number of uncertainties associated with the hydrodynamic drag estimates. For many of the gear components, their drag coefficients are estimated from experiments; (i) on idealized bodies that are similar to, but not exactly the same as the gear component (e.g. modelling a rope by a rigid cylinder); (ii) that occur in mid-water and do not include the influence of the seabed; (iii) where the component is towed directly through the water at an angle of attack of 90° and not at intermediate angles; or (iv) have different Reynolds number, surface roughness, and boundary flow regimes. The approach further assumes that the hydrodynamic drag of the individual gear components are additive and that there is no interference between them (Paschen *et al.*, 2000). All these factors will affect the hydrodynamics, and the corresponding drag estimates and sediment mobilization estimates must be used with caution.

Indeed, the validation of our approach showed, through comparison with literature estimates, that realistic hydrodynamic drag estimates were modelled for gear components, such as beam, shoes, wings, electrodes, tension relief cords, etc., that match the basic shapes for which empirically estimated parameters are available. However, further research is required to study the hydrodynamic drag of components such as the beam trawl net panels. The discrepancy between the modelled and measured drags may be due to the fact that the typical beam trawl towing speeds are greater than the maximum speed of about 4 knots ($2.1\ m\ s^{-1}$) in Reid's (1977) experimental data for otter trawls, and to the low headline of beam trawl nets, which means that the netting panels will be almost parallel to the towing direction. This differs from the otter trawl nets used by Reid (1977), whose netting panels will have a larger angle of attack and hence will be less streamlined and in turn will have a greater drag. In contrast, bottom net panels of beam trawls have chafers and/or dolly ropes to protect the net from wear. Chafers and dolly ropes were not included in the analysis, but may in turn increase the drag of beam trawl nets. The hydrodynamic drag of the cod-end will also depend on the catch size (O'Neill *et al.*, 2005). Hence, because pulse trawlers have a lower total catch volume than conventional beam trawlers (van Marlen *et al.*, 2014), the difference in hydrodynamic drag and sediment mobilization between both gear types is likely to be underestimated.

The accuracy of the model predictions will also be affected by the quality of the gear component data. The dimension of the various beam trawls in this paper have been presented to active fishers and gear manufacturers and we are confident that they are representative of the fleet, in particular for the pulse trawls (PUL) and the tickler chain beam trawls (TBT) used by large vessels. The sample size of the TBC and the TBT used by the small vessels was

limited rendering the quantitative results for these trawls less certain.

Although the hydrodynamic drag of the gear and the resulting sediment mobilization will be affected by the bottom currents, and this factor can be incorporated in our approach, we ignored this effect because the towing speed of $>2.5\ m\ s^{-1}$ of the beam trawl gear is substantially higher than the current speed in the southern North Sea ($\ll 0.8\ m\ s^{-1}$) https://odnature.naturalsciences.be/marine-forecasting-centre/en/maps/bottom_sea_water_velocity/nos (consulted 16 January 2021) (Aldridge *et al.*, 2015).

In spite of the limitations of our approach, our model-based estimates of the difference in the amount of sediment mobilized in the wake of a tickler chain beam trawl and a pulse trawl, showed good agreement with *in situ* field estimates (Depestele *et al.*, 2016). Further support comes from a recorded 33% reduction in fuel consumption by replacing tickler chains with electrodes (ICES, 2020) in comparison to a modelled reduction in hydrodynamic drag of 34%; and a field study of the biogeochemical impacts of pulse and tickler chain beam by Tiano *et al.* (2019) who showed in a comparative fishing experiment that tickler chain trawling reduced the sedimentary chlorophyll by 83% when compared to 43% obtained after pulse trawling. Hence, although there is uncertainty associated with some of the hydrodynamic drag estimates, we expect that our methodology provides a good approximation and will be particularly useful in capturing the relative differences between gears.

We are confident that our approach provides reasonable estimates of the quantity of sediment mobilized by different gears, which, as we have shown here, are particularly useful when used with information on different gear types, spatial and temporal fishing effort data and spatial sediment data, to estimate the differential impact of trawling at the fleet level. This will provide policymakers and fisheries managers with a quantitative means to assess the physical impacts of different fishing gears and fishing methods across sediment types. It will allow the ranking of gears in terms of their impact and permit a direct comparison with the physical impact of natural events (such as storms and tides) and of other uses of the seabed (such as mineral extraction and mining). Accordingly, it will permit a rationale and objective approach to fulfilling the requirements of the Common Fisheries Policy and the Marine Strategy Framework Directive. Our approach could also be used to provide estimates of trawling-induced sediment mobilization for mechanistic models of biogeochemical cycles (de Borger *et al.*, 2020) and hence, improve our understanding of trawling impacts on these processes. Furthermore, the hydrodynamic drag estimates will provide a better understanding of the forces required to tow a trawl gear across the seabed and contribute to the development of fuel-efficient gears that will reduce CO_2 and NO_x emissions by the fishing industry.

Supplementary data

Supplementary material is available at the ICESJMS online version of the manuscript.

Data Availability

Primary VMS-data and catch and effort data of the mandatory logbook are subject to confidential agreements. One should contact Sieto Verver, Head of the Centre for Fisheries Research (sieto.verver@wur.nl) for permission using these data. 'Technical Dossiers' (TD) of the pulse trawl vessels cannot be shared

publicly as the are privately owned. An excerpt of anonymised data will be shared on reasonable request to the corresponding author.

Acknowledgements

A. Lokker (Cooperatie Westvoorn), H. Klein-Woolthuis (HFK engineering), A. van Wijk (van Wijk, BV), M. Drijver and a number of individual skippers are gratefully acknowledged for providing information on gear dimensions. We thank Niels T. Hintzen for providing an updated data set with swept area ratios by grid cell for conventional tickler chain and chain mat beam trawl.

Funding

This study was funded by the European Maritime and Fisheries Fund (EMFF) and the Netherlands Ministry of Agriculture Nature and Food Quality (LNV) (Grand/Award Number: 1300021172), the Netherlands Ministry of Agriculture Nature and Food Quality (BO-code), the Belgian EMFF project “Benthisnationaal” and by the FP7-project BENTHIS (312088). The article does not necessarily reflect the views of the European Commission and does not anticipate the Commission’s future policy in this area.

References

- Aldridge, J. N., Parker, E. R., Bricheno, L. M., Green, S. L., and van der Molen, J. 2015. Assessment of the physical disturbance of the northern European Continental shelf seabed by waves and currents. *Continental Shelf Research*, 108: 121–140.
- Amoroso, R., Pitcher, C. R., Rijnsdorp, A. D., McConnaughey, R. A., Parma, A. M., Suuronen, P., Eigaard, O. R. *et al.* 2018. Bottom trawl-fishing footprints on the world’s continental shelves. *Proceedings of the National Academy of Science of the United States of America*, 115: E10275–E10282.
- Blom, W. C. 1982. Weerstand van boomkortuigen. Rijksinstituut voor Visserijonderzoek Report TO82-03. 42 pp.
- Blom, W. C. 1990. Weerstandcomponenten van een boomkortuig voor 1500 kW. Rijksinstituut voor Visserijonderzoek Report TO 90-01. 24 pp.
- Bolam, S. G., Garcia, C., Eggleton, J., Kenny, A. J., Buhl-Mortensen, L., Gonzalez-Mirelis, G., van Kooten, T. *et al.* 2017. Differences in biological traits composition of benthic assemblages between unimpacted habitats. *Marine Environmental Research*, 126: 1–13.
- Brent, R. 1973. *Algorithms for Minimization without Derivatives*. Prentice-Hall, Englewood Cliffs, NJ.
- Brylinsky, M., Gibson, J., and Gordon, D. C. Jr. 1994. Impacts of flounder trawls on the intertidal habitat and community of the Minas Basin, Bay of Fundy. *Canadian Journal of Fisheries and Aquatic Sciences*, 51: 650–661.
- Clark, M. R., Althaus, F., Schlacher, T. A., Williams, A., Bowden, D. A., and Rowden, A. A. 2016. The impacts of deep-sea fisheries on benthic communities: a review. *ICES Journal of Marine Science*, 73: i51–i69.
- Collie, J., Hiddink, J. G., Kooten, T. v., Rijnsdorp, A. D., Kaiser, M. J., Jennings, S., and Hilborn, R. 2017. Indirect effects of bottom fishing on the productivity of marine fish. *Fish and Fisheries*, 18: 619–637.
- de Borger, E., Tiano, J., Braeckman, U., Rijnsdorp, A. D., and Soetaert, K. 2020. Impact of bottom trawling on sediment biogeochemistry: a modelling approach. *Biogeosciences Discuss*, 2020: 1–32.
- de Groot, S., and Lindeboom, H. 1994. Environmental impact of bottom gears on benthic fauna in relation to natural resources management and protection of the North Sea. NIOZ Report 1994-11. RIVO-DLO Report C026/94. pp 257.
- de Haan, D., Fosseidengen, J. E., Fjellidal, P. G., Burggraaf, D., and Rijnsdorp, A. D. 2016. Pulse trawl fishing: characteristics of the electrical stimulation and the effect on behaviour and injuries of Atlantic cod (*Gadus morhua*). *ICES Journal of Marine Science*, 73: 1557–1569.
- Depestele, J., Degrendele, K., Esmaeili, M., Ivanović, A., Kröger, S., O’Neill, F. G., Parker, R. *et al.* 2019. Comparison of mechanical disturbance in soft sediments due to tickler-chain SumWing trawl vs. electro-fitted PulseWing trawl. *ICES Journal of Marine Science*, 76: 312–329.
- Depestele, J., Ivanović, A., Degrendele, K., Esmaeili, M., Polet, H., Roche, M., Summerbell, K. *et al.* 2016. Measuring and assessing the physical impact of beam trawling. *ICES Journal of Marine Science*, 73: i15–i26.
- Eigaard, O. R., Bastardie, F., Breen, M., Dinesen, G. E., Hintzen, N. T., Laffargue, P., Mortensen, L. O. *et al.* 2016. Estimating seabed pressure from demersal trawls, seines, and dredges based on gear design and dimensions. *ICES Journal of Marine Science*, 73: i27–i43.
- Eigaard, O. R., Bastardie, F., Hintzen, N. T., Buhl-Mortensen, L., Buhl-Mortensen, P., Catarino, R., Dinesen, G. E. *et al.* 2017. The footprint of bottom trawling in European waters: distribution, intensity, and seabed integrity. *ICES Journal of Marine Science*, 74: 847–865.
- Engelhard, G. H., 2008. One hundred and twenty years of change in fishing power of English North Sea trawlers. *In Advances in Fisheries Science 50 Years on from Beverton and Holt*, pp. 1–25. Ed. by A., Payne, J., Cotter, and T., Potter Blackwell Publishing, London.
- Ferro, R. S. T. 1981. *The Calculation of the Twin Area of a Trawl Net*, 5. Scottish Fisheries Information Pamphlets/Department of Agriculture and Fisheries for Scotland, Aberdeen, Scotland.
- Fonteyne, R., and Polet, H. 1992. *Huidige vistuigen en visserijmethoden in de Belgische Zeevisserij*. Rijkstation voor Zeevisserij, Oostende. 40 pp.
- Haasnoot, T., Kraan, M., and Bush, S. R. 2016. Fishing gear transitions: lessons from the Dutch flatfish pulse trawl. *ICES Journal of Marine Science*, 73: 1235–1243.
- Harris, P. T., and Baker, E. K. 2012. *Seafloor Geomorphology as Benthic Habitat*. Elsevier, London, UK. 900 pp.
- Hiddink, J. G., Jennings, S., Sciberras, M., Bolam, S., McConnaughey, R. A., Mazar, T., Hilborn, R. *et al.* 2019. The sensitivity of benthic macroinvertebrates to bottom trawling impacts using their longevity. *Journal of Applied Ecology*, 56: 1075–1084.
- Hiddink, J. G., Jennings, S., Sciberras, M., Szostek, C. L., Hughes, K. M., Ellis, N., Rijnsdorp, A. D. *et al.* 2017. Global analysis of depletion and recovery of seabed biota after bottom trawling disturbance. *Proceedings of the National Academy of Science of the United States of America*, 114: 8301–8306.
- Hintzen, N. T., Bastardie, F., Beare, D., Piet, G. J., Ulrich, C., Deporte, N., Egekvist, J. *et al.* 2012. VMStools: open-source software for the processing, analysis and visualisation of fisheries logbook and VMS data. *Fisheries Research*, 115–116: 31–43.
- Hoerner, S. F. 1965. *Fluid-dynamic drag*. Published by the author.
- Horwood, J. 1993. The Bristol Channel Sole (*Solea solea* (L))—a fisheries case-study. *Advances in Marine Biology*, 29: 215–367.
- ICES. 2020. ICES Working Group on Electrical Trawling (WGELECTRA). *ICES Scientific Reports*. 2:37. 108 pp. doi: 10.17895/ices.pub.6006. 115 pp.
- Jennings, S., and Kaiser, M. J. 1998. The effects of fishing on marine ecosystems. *Advances in Marine Biology*, 34: 201–352.
- Jones, J. B. 1992. Environmental impact of trawling on the seabed: a review. *New Zealand Journal of Marine and Freshwater Research*, 26: 59–67.
- Kaiser, M. J., Hilborn, R., Jennings, S., Amoroso, R., Andersen, M., Balliet, K., Barratt, E. *et al.* 2016. Prioritization of knowledge-needs

- to achieve best practices for bottom trawling in relation to seabed habitats. *Fish and Fisheries*, 17: 637–663.
- Lambert, G. I., Jennings, S., Hiddink, J. G., Hintzen, N. T., Hinz, H., Kaiser, M. J., and Murray, L. G. 2012. Implications of using alternative methods of vessel monitoring system (VMS) data analysis to describe fishing activities and impacts. *ICES Journal of Marine Science*, 69: 682–693.
- Lucchetti, A., and Sala, A. 2012. Impact and performance of Mediterranean fishing gear by side-scan sonar technology. *Canadian Journal of Fisheries and Aquatic Sciences*, 69: 1806–1816.
- Mayer, L. M., Schick, D. F., Findlay, R. H., and Rice, D. L. 1991. Effects of commercial dragging on sedimentary organic matter. *Marine Environmental Research*, 31: 249–261.
- Mazor, T., Pitcher, C. R., Rochester, W., Kaiser, M. J., Hiddink, J. G., Jennings, S., Amoroso, R. *et al.* 2021. Trawl fishing impacts on the status of seabed fauna in diverse regions of the globe. *Fish and Fisheries*, 22: 72–86.
- Mengual, B., Cayocca, F., Le Hir, P., Draye, R., Laffargue, P., Vincent, B., and Garlan, T. 2016. Influence of bottom trawling on sediment resuspension in the 'Grande-Vasière' area (Bay of Biscay, France). *Ocean Dynamics*, 66: 1181–1207.
- O'Neill, F. G., and Ivanović, A. 2016. The physical impact of towed demersal fishing gears on soft sediments. *ICES Journal of Marine Science*, 73: i5–i14.
- O'Neill, F. G., Knudsen, L. H., Wileman, D. A., and McKay, S. J. 2005. Cod-end drag as a function of catch size and towing speed. *Fisheries Research*, 72: 163–171.
- O'Neill, F. G., and Summerbell, K. 2011. The mobilisation of sediment by demersal otter trawls. *Marine Pollution Bulletin*, 62: 1088–1097.
- O'Neill, F. G., and Summerbell, K. J. 2016. The hydrodynamic drag and the mobilisation of sediment into the water column of towed fishing gear components. *Journal of Marine Systems*, 164: 76–84.
- Oberle, F. K. J., Storlazzi, C. D., and Hanebuth, T. J. J. 2016. What a drag: quantifying the global impact of chronic bottom trawling on continental shelf sediment. *Journal of Marine Systems*, 159: 109–119.
- Palanques, A., Puig, P., Guillén, J., Demestre, M., and Martín, J. 2014. Effects of bottom trawling on the Ebro continental shelf sedimentary system (NW Mediterranean). *Continental Shelf Research*, 72: 83–98.
- Paradis, S., Pusceddu, A., Masqué, P., Puig, P., Moccia, D., Russo, T., and Lo Iacono, C. 2019. Organic matter contents and degradation in a highly trawled area during fresh particle inputs (Gulf of Castellammare, southwestern Mediterranean). *Biogeosciences*, 16: 4307–4320.
- Paschen, M., Richter, U., and Kopnick, W. 2000. Trawl penetration in the seabed (TRAPESE). Final Report EC-Study Contract No 96-006. University of Rostock, Rostock, Germany: 150.
- Pitcher, C. R., Ellis, N., Jennings, S., Hiddink, J. G., Mazor, T., Kaiser, M. J., Kangas, M. I. *et al.* 2017. Estimating the sustainability of towed fishing-gear impacts on seabed habitats: a simple quantitative risk assessment method applicable to data-limited fisheries. *Methods in Ecology and Evolution*, 8: 472–480.
- Polet, H., and Depestele, J. 2010. Impact assessment of the effects of a selected range of fishing gears in the North Sea. ILVO Report. 110 pp., ILVO.
- Polymenakou, P. N., Pusceddu, A., Tselepidis, A., Polychronaki, T., Giannakourou, A., Fiordelmondo, C., and Hatziyanni, E. 2005. Benthic microbial abundance and activities in an intensively trawled ecosystem (Thermaikos Gulf, Aegean Sea). *Continental Shelf Research*, 25: 2570–2584.
- Poos, J. J., Hintzen, N. T., van Rijssel, J., and Rijnsdorp, A. D. 2020. Efficiency changes in bottom trawling for flatfish species as a result of the replacement of mechanical stimulation by electric stimulation. *ICES Journal of Marine Science*, 77: 2635–2645.
- Provoost, P., Braeckman, U., Van Gansbeke, D., Moodley, L., Soetaert, K., Middelburg, J. J., and Vanaverbeke, J. 2013. Modelling benthic oxygen consumption and benthic-pelagic coupling at a shallow station in the southern North Sea. *Estuarine, Coastal and Shelf Science*, 120: 1–11.
- Pusceddu, A., Bianchelli, S., Martín, J., Puig, P., Palanques, A., Masqué, P., and Danovaro, R. 2014. Chronic and intensive bottom trawling impairs deep-sea biodiversity and ecosystem functioning. *Proceedings of the National Academy of Science of the United States of America*, 111: 8861–8866.
- Pusceddu, A., Fiordelmondo, C., Polymenakou, P., Polychronaki, T., Tselepidis, A., and Danovaro, R. 2005. Effects of bottom trawling on the quantity and biochemical composition of organic matter in coastal marine sediments (Thermaikos Gulf, northwestern Aegean Sea). *Continental Shelf Research*, 25: 2491–2505.
- Reid, A. J. 1977. A net drag formula for pelagic nets. *Scottish Fisheries Research Report*. Number 7. 12 pp.
- Rhoads, D. C. 1974. Organisms-sediment relations on the muddy sea floor. *Oceanography and Marine Biology Annual Review*, 12: 263–300.
- Rijnsdorp, A. D., Bolam, S. G., Garcia, C., Hiddink, J. G., Hintzen, N., van Denderen, P. D., and van Kooten, T. 2018. Estimating the sensitivity of seafloor habitats to disturbance by bottom trawl fisheries based on the longevity of benthic fauna. *Ecological Applications*, 28: 1302–1312.
- Rijnsdorp, A. D., Depestele, J., Eigaard, O. R., Hintzen, N. T., Ivanovic, A., Molenaar, P., O'Neill, F. G. *et al.* 2020a. Mitigating seafloor disturbance of bottom trawl fisheries for North Sea sole *Solea solea* by replacing mechanical with electrical stimulation. *PLoS One*, 8: e61357.
- Rijnsdorp, A. D., Hiddink, J. G., van Denderen, P. D., Hintzen, N. T., Eigaard, O. R., Valanko, S., Bastardie, F. *et al.* 2020b. Different bottom trawl fisheries have a differential impact on the status of the North Sea seafloor habitats. *ICES Journal of Marine Science*, 77: 1772–1786.
- Rijnsdorp, A. D., Poos, J. J., Quirijns, F. J., HilleRisLambers, R., de Wilde, J. W., and Den Heijer, W. M. 2008. The arms race between fishers. *Journal of Sea Research*, 60: 126–138.
- Sangster, G. I., and Breen, M. 1998. Gear performance and catch comparison trials between a single trawl and a twin rigged gear. *Fisheries Research*, 36: 15–26.
- Sciberras, M., Hiddink, J. G., Jennings, S., Szostek, C. L., Hughes, K. M., Kneafsey, B., Clarke, L. *et al.* 2018. Response of benthic fauna to experimental bottom fishing: a global meta-analysis. *Fish and Fisheries*, 19: 698–715.
- Sciberras, M., Parker, R., Powell, C., Robertson, C., Kröger, S., Bolam, S., and Hiddink, J. G. 2016. Impacts of bottom fishing on the sediment infaunal community and biogeochemistry of cohesive and non-cohesive sediments. *Limnology and Oceanography*, 61: 2076–2089.
- Soetaert, K., and Middelburg, J. J. 2009. Modeling eutrophication and oligotrophication of shallow-water marine systems: the importance of sediments under stratified and well-mixed conditions. *In Eutrophication in Coastal Ecosystems*, pp. 239–254. Ed. by J. H. Andersen and D. J. Conley. Springer, Dordrecht.
- Soetaert, M., Boute, P. G., and Beaumont, W. R. C. 2019. Guidelines for defining the use of electricity in marine electrotrawling. *ICES Journal of Marine Science*, 76: 1994–2007.
- Soetaert, M., Decostere, A., Polet, H., Verschuere, B., and Chiers, K. 2015. Electrotrawling: a promising alternative fishing technique warranting further exploration. *Fish and Fisheries*, 16: 104–124.
- Soetaert, M., Decostere, A., Verschuere, B., Saunders, J., Van Caelenberge, A., Puvanendran, V., Mortensen, A. *et al.* 2016. Side-effects of electrotrawling: exploring the safe operating space for Dover sole (*Solea solea* L.) and Atlantic cod (*Gadus morhua* L.). *Fisheries Research*, 177: 95–103.

- Taal, C., and Klok, A. J. 2014. Pulswing; Ontwikkeling van een vistuig voor platvis waarin puls-techniek met de SumWing is gecombineerd. LEI Report 2014-039. 46 pp.
- Tang, H., Hu, F., Xu, L., Dong, S., Zhou, C., and Wang, X. 2019. Variations in hydrodynamic characteristics of netting panels with various twine materials, knot types, and weave patterns at small attack angles. *Scientific Reports*, 9: 1923.
- Tiano, J. C., Witbaard, R., Bergman, M. J. N., van Rijswijk, P., Tramper, A., van Oevelen, D., and Soetaert, K. 2019. Acute impacts of bottom trawl gears on benthic metabolism and nutrient cycling. *ICES Journal of Marine Science*, 76: 1917–1930.
- Trimmer, M., Petersen, J., Sivyer, D. B., Mills, C., Young, E., and Parker, E. R. 2005. Impact of long-term benthic trawl disturbance on sediment sorting and biogeochemistry in the southern North Sea. *Marine Ecology Progress Series*, 298: 79–94.
- van de Velde, S., Van Lancker, V., Hidalgo-Martinez, S., Berelson, W. M., and Meysman, F. J. 2018. Anthropogenic disturbance keeps the coastal seafloor biogeochemistry in a transient state. *Scientific Reports*, 8: 1–10.
- Wolfshaar, K. E., Denderen, P. D., Schellekens, T., and Kooten, T. 2020. Food web feedbacks drive the response of benthic macrofauna to bottom trawling. *Fish and Fisheries*, 21: 962–972.
- van Marlen, B., van Keeken, O. A., Dijkman Dulkes, H. J. A., Groeneveld, K., Pasterkamp, T. L., de Vries, M., and Westerink, H. J. 2009. Vergelijking van vangsten en brandstofverbruik van kotters vissend met conventionele en SumWing-boomkorren. Wageningen IMARES Rapport C023/09. 38 pp.
- van Marlen, B., Wiegerinck, J. A. M., van Os-Koomen, E., and van Barneveld, E. 2014. Catch comparison of flatfish pulse trawls and a tickler chain beam trawl. *Fisheries Research*, 151: 57–69.
- Watling, L., Findlay, R. H., Mayer, L. M., and Schick, D. F. 2001. Impact of a scallop drag on the sediment chemistry, microbiota, and faunal assemblages of a shallow subtidal marine benthic community. *Journal of Sea Research*, 46: 309–324.
- Wilson, R. J., Speirs, D. C., Sabatino, A., and Heath, M. R. 2018. A synthetic map of the north-west European Shelf sedimentary environment for applications in marine science. *Earth System Science Data*, 10: 109–130.
- Xu, Z., and Huang, S. 2014. Numerical investigation of mooring line damping and the drag coefficients of studless chain links. *Journal of Marine Science and Application*, 13: 76–84.
- Zhou, C., Xu, L. X., Hu, F. X., and Qu, X. Y. 2015. Hydrodynamic characteristics of knotless nylon netting normal to free stream and effect of inclination. *Ocean Engineering*, 110: 89–97.

Handling editor: Michael Pol